ISSN 0925-8388
VOLUME 1000 | 30 JULY 2022

JOURNAL OF ALLOYS AND COMPOUNDS

materialstoday

ScienceDirect

Journal of Alloys and Compounds

Supports *open access*

7.6 CiteScore

4.65 Impact Factor

Menu

Search in this journal

Submit your article

Guide for authors

About the journal

Aims and scope | Editorial board | Abstracting and indexing

Editor-in-Chief

Senior Editors

Daria Drozdenko
Charles University Faculty of Mathematics and Physics Department of Physics of Materials, 3 Ke Karlovu, 121 16, Praha, Czech Republic
Analysis of plastic deformation in metals by acoustic emission (AE) technique., Complex study of Mg alloys (including Mg-LPSO-based alloys), microstructure and mechanical properties, Advanced techniques for microstructure analysis

Dmitry G. Eskin
Brunel University Brunel Centre for Advanced Solidification Technology, UB8 3PH, Uxbridge, United Kingdom
structure refinement, degassing, exfoliation, metal processing, solidification

Huiqing Fan
Northwestern Polytechnical University School of Materials Science and Engineering, 127 Youyixilu, 710072, Xian, China
Functional Ceramics, Nano Materials, Thin Films

Josef Fidler
TU Wien Institute of Solid State Physics, Wiedner Hauptstrasse 8-10, 1040, Wien, Austria

Thiagarajan Gnanasekaran
Indira Gandhi Centre for Atomic Research, Indira Gandhi Centre for Atomic Research,Kalpakkam, 603102, Kalpakkam, India
Phase Diagrams; Measurement of Thermochemical Properties; Solid State Ionics; Chemical Sensors and Sensor Materials; Hydrogen in Metals; Chemical Synthesis of Inorganic Compounds

Mohamed Henini
University of Nottingham School of Physics and Astronomy, University Park, NG7 2RD, Nottingham, United Kingdom
Low Dimensional Structures and Devices, Nanotechnoloy and Nanoscience, Self-Assembled Semiconductor Nanostructures, Semiconductor Materials, III-V Electronic and Optoelectronic Devices, Photovoltaic Materials and Devices, Molecular Beam Epitaxy, Deep Level Transient Spectroscopy

Jacques Huot
University of Quebec in Trois Rivieres Hydrogen Research Institute, 3351 Boulevard Des Forges (P.O. Box 500), Trois Rivieres, G9A 5H7, Quebec, Canada
Hydrogen research, Hydrogen storage, Metal hydrides, Gas-solid interactions, Materials characterization, Neutron diffraction, Materials synthesis

Li Jin
Shanghai Jiao Tong University School of Materials Science and Engineering, 1954 Hua Shan Road, 2000030, Shanghai, China
Texture of Mg alloys, Texture induced deformation behaviour, Metal forming, Application of light alloys

Yongchang Liu
Tianjin University, 300072, Tianjin, China

Solid-state phase transformations: thermodynamic and kinetic analyses; rapid solidification; metal-activated sintering and Microstructural control in ni(co)-based superalloys, heat-resistance steels, superconducting materials, lead-free solders and ti-al intermetallic compounds.

Nicoleta Lupu
National Institute of Research and Development for Technical Physics, Mangeron Av 47, 6600, Iaşi, Romania
Metallic glasses; Bulk metallic glasses; Magnetic and magnetoelectric materials; Magnetoelastic processes; sensors and devices; Physics and chemistry of surfaces and interfaces; Nanoparticles and nanowire arrays; Hydrogen storage materials.

Valmor Mastelaro
University of Sao Paulo Campus of Sao Carlos, Sao Carlos, Brazil
Structure-property relationships, ZnO Based Materials, Metal Oxide Gas sensors, Glass and Glass-Ceramics, Metal oxide thin films, XAS and XPS spectroscopies

BS Murty
Indian Institute of Technology Hyderabad, IITH Main Road, Near NH-65, Sangareddy, 502285, Kandi, India
Physical metallurgy, alloy design, Phase transformations, High entropy alloys, bulk metallic glasses, nanocrystalline materials, metal matrix composites, electron microscopy, atom probe tomography.

Hari Srikanth
University of South Florida Department of Physics, 4202 E Fowler Ave, Tampa, Florida, FL 33620, United States
Magnetism and magnetic materials, Nanostructured materials for energy and biomedical applications, Structure-property correlations in functional materials, Strongly correlated systems

Wieslaw Strek
Institute of Low Temperature and Structure Research Polish Academy of Sciences, Okólna str. 2, 50-422, Wroclaw, Poland
Rare earth ions and transition metal ions, doped sol-gel materials, photonic structures, nanomaterials, nanoceramics and crystals.

Isabel Van Driessche
Ghent University Department of Chemistry, Krijgslaan 281 (Building S3), 9000, Gent, Belgium
Chemical Solution deposition (CSD, ink jet printing) of ceramics. Materials of interest : superconducting perovskites and buffer layers for production of coated conductors, titanates for (photo)catalytic and battery applications, low-E coatings; Formulation of environmentally friendly based inks. Use of bottom-up chemical synthesis approaches (hydrothermal, microwave-assisted, hot injection) for the synthesis of ceramic nanoparticles/suspensions.

Mingzhong Wu
Colorado State University Department of Physics, 1875 Campus Delivery, Fort Collins, Colorado, CO 80523, United States
Experimental Condensed Matter: Magnetism, Magnetic Materials, Spintronics, and Spin Caloritronics

Renbing Wu
Fudan University Department of Material Science, 200433, Shanghai, China
Semiconductor, Transition Metal-based composites, Electrode materials for energy storage and conversion

Xuezhang Xiao
Zhejiang University School of Materials Science and Engineering, 38 Zheda Road, Hangzhou, China

Volodymyr Yartys
Institute for Energy Technology, 2027, Kjeller, Norway
Nanomaterials for energy storage. Rechargeable Batteries. Hydrogen as an Energy Carrier. New Intermetallics and Carbon Materials for Hydrogen Storage and Battery Applications. Synchrotron and neutron powder diffraction. Crystal structures of novel materials.

Editorial Advisory Board

G. Adachi
Osaka, Japan
Chemistry and materials science of rare earths, Solid state electrochemistry

A.V. Andreev
Praha, Czech Republic
Magnetism of rare-earth and uranium intermetallics, Crystal structure of rare-earth and uranium intermetallics, Metallic hydrides, Permanent magnets

A. Dahle
Jonkoping, Sweden
Solidification, Rheology, Light alloys, Lead-free soldering, Hydrogen storage

F.J. Di Salvo
Ithaca, New York, United States
Synthesis and characterization of solid state compounds, novel crystal structures. Physical properties such as electrical resistivity, thermal conductivity, thermopower.

T.B. Flanagan
Burlington, Vermont, United States
Hydrogen diffusion through metals and alloys, Thermodynamics of H metal systems, Characterization of intermetallic-H systems

C. Gomez Polo
Pamplona, Spain
Magnetism; magnetic nanoparticles and nanostructured magnetic materials; transition metal oxides

J.-M. Greneche
Le Mans, France

V.G. Harris
Boston, Massachusetts, United States
Magnetoceramics, principally ferrites, rf materials, magnetism

Hsiang Hsing-I, PhD
National Cheng Kung University College of Engineering, Tainan, Taiwan
Ceramic processing, Electroceramics, CIGS/CZTS, Powder synthesis

D.C. Johnson
Eugene, Oregon, United States
Solid state chemistry, Thermoelectric materials, X-ray reflectivity, Thermal conductivity, Electrical transport

H. Kleinke
Waterloo, Ontario, Canada
Solid state chemistry, materials chemistry, energy conversion, thermoelectric materials, transport properties, electronic structure calculations, crystal structures, chalcogenides, pnictides

E.J. Mittermeijer
Stuttgart, Germany
Phase transformations, (interface) thermodynamics and kinetics; Nanomaterials, their unusual properties; Stress and phase transformations in (very) thin (multi)layers; surface engineering (nitriding and nitrocarburizing of iron, iron alloys and steels); oxidation of metals and alloys

Y. Mozharivskyj
Hamilton, Ontario, Canada
Thermoelectric materials, Magnetocaloric materials, X-ray analysis

R. Nesper
Zurich, Switzerland
Inorganic chemistry, Zintl phases, nanoscience, intermetallic phases, electrochemistry, hard materials.

E. Peterson
Los Alamos, New Mexico, United States
Actinide thermodynamics and equilibrium phase diagrams, High temperature superconductor synthesis, characterization, and applications, Carbon nanotubes, Radiation damage, and Vaporization studies

W. Prellier
Caen, France

K. Z. Rožman
Ljubljana, Slovenia

H. Sakaguchi
Tottori, Japan
Li ion materials, Hydrogen storage materials, hydrides

H. Sato
Tokyo, Japan

O.N. Senkov
Dayton, Ohio, United States

K. Suzuki
Miyagi, Japan

T. Takabatake
Higashihiroshima, Japan

T. Yamase
Yokohama, Japan
Catalysis, photoluminescence.

C.-L. Yeh
Taichung, Taiwan
Self-propagating High-temperature Synthesis (SHS), Transition metal borides and nitrides, Intermetallics, MAX phases, Thermite Reaction

All members of the Editorial Board have identified their affiliated institutions or organizations, along with the corresponding country or geographic region. Elsevier remains neutral with regard to any jurisdictional claims.

ISSN: 0925-8388

Journal of Alloys and Compounds
Supports *open access*

7.6
CiteScore

Volume 844

5 December 2020

Previous vol/issue Next vol/issue

Full text access

Editorial Board

Article 156647

Download PDF

Research article ○ Abstract only

Improved solid-state synthesis and electrochemical properties of $LiNi_{0.6}Mn_{0.2}Co_{0.2}O_2$ cathode materials for lithium-ion batteries

Luyang Wang, Bin Huang, Weixiong Xiong, Meng'en Tong, ... Jianwen Yang

Article 156034

Purchase PDF Article preview

Research article ○ Abstract only

Primary solidification of ternary compounds in Al-rich Al–Ce–Mn alloys

Y. Yang, S. Bahl, K. Sisco, M. Lance, ... R.R. Dehoff

Article 156048

Purchase PDF Article preview

Research article ○ Abstract only

Bi_2S_3–CoS@C core- shell structure derived from ZIF-67 as anodes for high performance lithium-ion batteries

Xiangju Chen, Peng Wang, Zhiwei Zhang, Longwei Yin

Journal of Alloys and Compounds
Supports *open access*

7.6
CiteScore

Articles & Issues About Publish

Research article ○ Abstract only
Strongly luminescent and highly stable core-shell suprastructures from *in-situ* growth of $CsPbBr_3$ perovskite nanocrystals in multidentate copolymer micelles
Aizhao Pan, Lihe Yan, Xiaoqin Ma, Youshen Wu, ... Ling He
Article 156102
Purchase PDF Article preview

Research article ○ Abstract only
Efficient near-infrared laser emission and nonlinear optical properties of a newly developed Yb:LYSB laser crystal
Alin Broasca, Madalin Greculeasa, Flavius Voicu, Stefania Hau, ... Lucian Gheorghe
Article 156143
Purchase PDF Article preview

Research article ○ Abstract only
Thermodynamic and kinetic studies of the Cu–Zr–Al(–Sn) bulk metallic glass-forming system
Hao-Ran Jiang, Benedikt Bochtler, Sascha S. Riegler, Xian-Shun Wei, ... Jun Shen
Article 156126
Purchase PDF Article preview

Research article ○ Abstract only
Structural, Mössbauer studies and oxygen permeation characteristics of $Sr_{1-x}Ba_xFe_{1-y}Li_yO_{3-\xi}$ (x = 0, 0.5; y = 0 – 0.10) system
Shivendra Kumar Jaiswal, Rajeev Ranjan, Jitendra Kumar
Article 155832
Purchase PDF Article preview

Research article ○ Abstract only
Reversible photochromism for the enhancement of carrier separation in $Zn_{1-x}Cu_xS$
Peiwen Lv, Chaosheng Xu, Jiajia Huang, Chengjiang Du, Feng Huang
Article 155880
Purchase PDF Article preview

Research article ○ Abstract only
Engineering mixed polyanion red-emitting $Rb_2Bi(PO_4)(WO_4):Eu^{3+}$ phosphors with negligible thermal quenching and high quantum yield
Zhen Jia, Xiuling Zhang, Xiaoying Hua, Yan Dong, ... Mingjun Xia
Article 155875
Purchase PDF Article preview

Journal of Alloys and Compounds
Supports *open access*

7.6
CiteScore

H.W. Chang, S.U. Jen, D.H. Tseng, Y.H. Liao, ... W.C. Chang
Article 156086

Purchase PDF Article preview

Research article ○ Abstract only
Hydrophilic $Ni(OH)_2$@CoB nano-chains with shell-core structure as an efficient catalyst for oxygen evolution reaction
Jun Lu, Shan Ji, Palanisamy Kannan, Hui Wang, ... Rongfang Wang
Article 156129

Purchase PDF Article preview

Research article ○ Abstract only
Ultra-high-Q and wide temperature stable $Ba(Mg_{1/3}Ta_x)O_3$ microwave dielectric ceramic for 5G-oriented dielectric duplexer adhibition
Lizheng Ni, Lingxia Li, Mingkun Du
Article 156106

Purchase PDF Article preview

Research article ○ Abstract only
Chemical stabilization of Eu^{2+} in $LuPO_4$ and YPO_4 hosts and its peculiar sharp line luminescence
Justyna Zeler, Megi Sulollari, Andries Meijerink, Marco Bettinelli, Eugeniusz Zych
Article 156096

Purchase PDF Article preview

Research article ○ Abstract only
Structure and phase transformations in scandia, yttria, ytterbia and ceria-doped zirconia-based solid solutions during directional melt crystallization
Mikhail A. Borik, Mikhail V. Gerasimov, Alexey V. Kulebyakin, Nataliya A. Larina, ... Nataliya Yu Tabachkova
Article 156040

Purchase PDF Article preview

Research article ○ Abstract only
Morphology controlled synthesis of $Ba_4Bi_3F_{17}:Er^{3+},Yb^{3+}$ and the dual-functional temperature sensing and optical heating applications
Peng Liu, Jiaqiang Liu, Youwen Zhang, Zhiguo Xia, Yan Xu
Article 156116

Purchase PDF Article preview

Research article ○ Abstract only
Superior catalytic effect of facile synthesized $LaNi_{4.5}Mn_{0.5}$ submicro-particles on the hydrogen storage properties of MgH_2

Journal of Alloys and Compounds
Supports *open access*

7.6
CiteScore

Articles & Issues About Publish

Purchase PDF Article preview

Research article ○ Abstract only
Study on deformation behavior in supercooled liquid region of a Ti-based metallic glassy matrix composite by artificial neural network
Y.S. Wang, R.K. Linghu, W. Zhang, Y.C. Shao, ... J. Xu
Article 155761

Purchase PDF Article preview

Research article ○ Abstract only
Isothermal oxidation and TGO growth behavior of NiCoCrAlY-YSZ thermal barrier coatings on a Ni-based superalloy
Jiaqi Shi, Tiebang Zhang, Bing Sun, Bing Wang, ... Lin Song
Article 156093

Purchase PDF Article preview

Research article ○ Abstract only
Combustion procedure deposited SnO_2 electron transport layers for high efficient perovskite solar cells
Jinbiao Jia, Jia Dong, Jihuai Wu, Haoming Wei, Bingqiang Cao
Article 156032

Purchase PDF Article preview

Research article ○ Abstract only
Type-II superconductivity below 4K in $Sn_{0.4}Sb_{0.6}$
M.M. Sharma, Kapil Kumar, Lina Sang, X.L. Wang, V.P.S. Awana
Article 156140

Purchase PDF Article preview

Research article ○ Abstract only
Improving the amorphous forming ability and magnetic properties of FeSiBPCu amorphous and nanocrystalline alloys by utilizing carbon
Y.L. Li, Z.X. Dou, X.M. Chen, K. Lv, ... X.D. Hui
Article 155767

Purchase PDF Article preview

Research article ○ Abstract only
Electrocaloric effect of alkali co-substituted $Sr_{0.6}Ba_{0.4}Nb_2O_6$ ceramics
Arif Kurnia, Emriadi, Nandang Mufti, Zulhadjri, Umut Adem
Article 156132

Purchase PDF Article preview

Journal of Alloys and Compounds
Supports *open access*

7.6
CiteScore

photocatalytic degradation of organic dyes
N.F. Andrade Neto, A.B. Lima, M.R.D. Bomio, F.V. Motta
Article 156077

Purchase PDF Article preview

Research article ○ Abstract only
The pitch-based silicon-carbon composites fabricated by electrospraying technique as the anode material of lithium ion battery
Chih-Yu Chen, Ai-Hua Liang, Cheng-Liang Huang, Ting-Hao Hsu, Yuan-Yao Li
Article 156025

Purchase PDF Article preview

Research article ○ Abstract only
Growth mechanism of MnS/Fe on TiN surface: First principle investigation
Qianren Tian, Jie Li, Xiangyu Wu, Jianxun Fu, Guocheng Wang
Article 155831

Purchase PDF Article preview

Research article ○ Abstract only
Oxygen vacancies and F^+ centre tailored room temperature ferromagnetic properties of CeO_2 nanoparticles with Pr doping concentrations and annealing in hydrogen environment
H.R. Khakhal, Sudhish Kumar, S.N. Dolia, B. Dalela, ... S. Dalela
Article 156079

Purchase PDF Article preview

Research article ○ Abstract only
Heterostructure Co_3O_4@$NiWO_4$ nanocone arrays with enriched active area for efficient hydrogen evolution reaction
Xiuhua Wang, Peng He, Yuan Yang, Yaoyao Pan, ... Rene Ling
Article 156095

Purchase PDF Article preview

Research article ○ Abstract only
Core-shell structured $CuCo_2S_4$@$CoMoO_4$ nanorods for advanced electrode materials
Xiaoqi Mao, Ying Wang, Cuili Xiang, Dan Zhan, ... Yongjin Zou
Article 156133

Purchase PDF Article preview

Research article ○ Abstract only
Analysis of damage-tolerance of TRIP-assisted $V_{10}Cr_{10}Fe_{45}Co_{30}Ni_5$ high-entropy alloy at room and cryogenic temperatures
Yong Hee Jo, Junha Yang, Kyung-Yeon Doh, Woojin An, ... Sunghak Lee

Journal of Alloys and Compounds
Supports *open access*

7.6
CiteScore

Articles & Issues About Publish

Purchase PDF Article preview

Correspondence ○ Abstract only
Novel approach to copper sintering using surface enhanced brass micro flakes for microelectronics packaging
Sri Krishna Bhogaraju, Fosca Conti, Hiren R. Kotadia, Simon Keim, ... Gordon Elger
Article 156043

Purchase PDF Article preview

Research article ○ Abstract only
Computational, MD simulation, SEM/EDX and experimental studies for understanding adsorption of benzimidazole derivatives as corrosion inhibitors in 1.0 M HCl solution
E. Ech-chihbi, A. Nahlé, R. Salim, F. Benhiba, ... A. Zarrouk
Article 155842

Purchase PDF Article preview

Research article ○ Abstract only
Phase inversion synthesis of Fe_3O_4@NC composites with superior lithium storage performance
Shuai Ru, Xia Wang, Guoqing Ma, Junyu Tan, ... Zhaoquan Ai
Article 156039

Purchase PDF Article preview

Research article ○ Abstract only
A novel long-period phase in $Mg_{97}Yb_2Cu_1$ alloy
Teruki Tsuchiya, Masahiro Fukuda, Hiroaki Ohfuji, Michiaki Yamasaki, ... Masafumi Matsushita
Article 155972

Purchase PDF Article preview

Research article ○ Abstract only
Microstructure and mechanical properties of Mo–Cu–Zr composites fabricated via microwave sintering
Rui Shu, Xiaosong Jiang, Y.X. Zhang, Richard Wuhrer, ... Zhiping Luo
Article 156120

Purchase PDF Article preview

Research article ○ Abstract only
Electrochemical behavior of nanostructured NiO@C anode in a lithium-ion battery using $LiNi_{1/3}Co_{1/3}Mn_{1/3}O_2$ cathode
Shuangying Wei, Daniele Di Lecce, Rosaria Brescia, Giammarino Pugliese, ... Jusef Hassoun
Article 155365

Purchase PDF Article preview

Journal of Alloys and Compounds
Supports *open access*

7.6
CiteScore

Przemysław Sedzicki, Łukasz Skowroński, Robert Szczesny, Hans-Werner Becker, ... Beata Derkowska-Zielińska
Article 156002

Purchase PDF Article preview

Research article ○ Abstract only
Biomolecule assisted morphology-controllable synthesis of Zinc Sulphide nanomaterials for efficient photocatalytic activity under solar irradiation
Dhrubajyoti Samanta, Parita Basnet, T. Inakhunbi Chanu, Somenath Chatterjee
Article 155810

Purchase PDF Article preview

Research article ○ Abstract only
Effect of pressure on the phase stability and magnetostructural transitions in nickel-rich NiFeGa ribbons
A.F. Manchón-Gordón, J.J. Ipus, M. Kowalczyk, A. Wójcik, ... A. Conde
Article 156092

Purchase PDF Article preview

Research article ○ Abstract only
Effect of RE on accelerating the kinetics of boride layer growth on titanium alloy
Yan song Zhu, Yu xuan Yin, Jun Wu, Yun fei Liu, ... Tae Jo Ko
Article 156091

Purchase PDF Article preview

Research article ○ Abstract only
Structural, elastic, electronic and hardness properties of osmium diboride predicted from first principles calculations
Shiquan Feng, Yang Yang, Feng Guo, Lei Su, ... Kun Yang
Article 156098

Purchase PDF Article preview

Research article ○ Abstract only
Structural and magnetic properties of the interstitial carbide-hydride $NdScSiC_{0.5}H_{0.2}$
Tadhg Mahon, Etienne Gaudin, Vivian Nassif, Sophie Tencé
Article 156105

Purchase PDF Article preview

Research article ○ Abstract only
A new class of mixed-valent europium halide *ortho*-oxoborates: $Eu_6X[BO_3]_4$ (X = Cl and Br)
Christian Funk, Olaf Reckeweg, Francis J. DiSalvo, Armin Schulz, ... Thomas Schleid
Article 156038

Journal of Alloys and Compounds
Supports *open access*

7.6
CiteScore

Articles & Issues About Publish

Research article ○ Abstract only
Multiple ratiometric thermometry: Enhanced sensing behaviour via Stark sublevels
Manisha Mondal, Vineet Kumar Rai
Article 155914
Purchase PDF Article preview

Research article ○ Abstract only
Efficient capturing and oxidation of CO through bimetallic surface alloying on WC (0001)
Yuling Zhao, Xilin Zhang, Zongxian Yang
Article 156125
Purchase PDF Article preview

Research article ○ Abstract only
Synergistic optimization of the thermoelectric properties of $Zn_{0.98}Al_{0.02}O$ using high-pressure and high-temperature treatment
Qi Chen, Hongan Ma, Xinjian Li, Yao Wang, ... Xiaopeng Jia
Article 156124
Purchase PDF Article preview

Research article ○ Abstract only
Synthesis of bilayer MoS_2 nanosheets by green chemistry approach and its application in triboelectric and catalytic energy harvesting
Srikanta Karmakar, Rajat Sarkar, Chandra Sekhar Tiwary, Pathik Kumbhakar
Article 155690
Purchase PDF Article preview

Research article ○ Abstract only
Magnetic properties of $Sr_{0.7}R_{0.3}CoO_{3-\delta}$ (R = Tb, Er and Ho) perovskites
V. Cascos, J.L. Martínez, M.T. Fernández-Díaz, J.A. Alonso
Article 156121
Purchase PDF Article preview

Research article ○ Abstract only
Simulation and parameter identification based on electrochemical- thermal coupling model of power lithium ion-battery
Yu Liu, Shui Tang, Lixiang Li, Fangyang Liu, ... Huijun Gu
Article 156003
Purchase PDF Article preview

Research article ○ Abstract only
Crystal growth, structural characteristics and electronic structure of $Ba_{1-x}Pb_xFe_{12}O_{19}$ (x = 0.23–0.80) hexaferrites

Journal of Alloys and Compounds
Supports *open access*

7.6
CiteScore

Articles & Issues About Publish

Purchase PDF Article preview

Research article ○ Abstract only
Systematic studies on $Ca_{19}M_2(PO_4)_{14}:Eu^{3+}$ (M = Mg, Zn) phosphors: Effects of M cation on photoluminescence
Ya-jie Han, Shuang Wang, Han Liu, Lei Shi, ... Shao-li Niu
Article 156070

Purchase PDF Article preview

Research article ○ Abstract only
In-situ visualization of corrosion behavior of $Al_xCoCrFeNi$ high-entropy alloys during electrochemical polarization
Yunzhu Shi, Jingke Mo, Feng-Yuan Zhang, Bin Yang, ... Ying Zhao
Article 156014

Purchase PDF Article preview

Research article ○ Abstract only
A promising biomimetic surface enhances cell proliferation and adhesion ability for promoting early-stage osseointegration
Fang-Yu Fan, Chia-Jen Wu, Yung-Chieh Cho, Erwan Sugiatno, ... Mao-Suan Huang
Article 155905

Purchase PDF Article preview

Research article ○ Abstract only
Characterization of electrodeposited Ni–Cr/hBN composite coatings
Mehmet Demir, Erdoğan Kanca, İsmail Hakki Karahan
Article 155511

Purchase PDF Article preview

Research article ○ Abstract only
Investigation of dehydrogenation of Ti–V–Cr alloy by using in-situ neutron diffraction
Viney Dixit, Lambert van Eijck, Jacques Huot
Article 156130

Purchase PDF Article preview

Research article ○ Abstract only
"Magic mitt": Morphologically controllable AuAg@AuAg yolk-shell nanostars with better plasmonic optical properties
Yun-le Li, Jian Zhu, Guo-jun Weng, Jian-jun Li, ... Jun-wu Zhao
Article 156134

Purchase PDF Article preview

Research article ○ Abstract only

Journal of Alloys and Compounds
Supports *open access*

7.6
CiteScore

Articles & Issues About Publish

Purchase PDF Article preview

Research article ○ Abstract only
Mapping thermoelectric properties of polycrystalline *n*-type $Bi_2Te_{3-x}Se_x$ alloys by composition and doping level
Sung-Jin Jung, Byeong-Hyeon Lee, Sung Ok Won, Seong Keun Kim, ... Seung-Hyub Baek
Article 155828

Purchase PDF Article preview

Research article ○ Abstract only
A rational interpretation of solidification microstructures in the Mg-rich corner of the Mg–Al–La system
Manjin Kim, Stuart D. McDonald, Trevor B. Abbott, Mark A. Easton, ... Kazuhiro Nogita
Article 156068

Purchase PDF Article preview

Research article ○ Abstract only
Structural and electromagnetic properties of Fe_2Co-multi-walled carbon nanotubes-polystyrene based composite
Mariya A. Kazakova, Sergey I. Moseenkov, Georgiy V. Golubtsov, Evgeniy Yu Korovin, ... Vladimir L. Kuznetsov
Article 156107

Purchase PDF Article preview

Research article ○ Abstract only
Morphology–controlled synthesis of the porous Co_3O_4 with rugby–shaped and spherical structures and theirs electrochemical properties as negative materials for Li–ion batteries
Jian Chen, Na Zhao, Yinggang Zhao, Ji Hu, ... Zhongyuan Zhang
Article 156058

Purchase PDF Article preview

Research article ○ Abstract only
Boosted photocatalytic Cr(VI) reduction over Z-scheme MIL-53(Fe)/$Bi_{12}O_{17}Cl_2$ composites under white light
Hua Li, Chen Zhao, Xia Li, Huifen Fu, ... Chong-Chen Wang
Article 156147

Purchase PDF Article preview

Research article ○ Abstract only
A novel raspberry-like yolk-shell structured Si/C micro/nano-spheres as high-performance anode materials for lithium-ion batteries
Canliang Ma, Zairan Wang, Yun Zhao, Yong Li, Jing Shi
Article 156201

Journal of Alloys and Compounds
Supports *open access*

7.6
CiteScore

Correspondence ○ Abstract only
$NaSn_2(PO_4)_3$ submicro-particles for high performance Na/Li mixed-ion battery anodes
Beibei Zhao, Xudong Zhang, Guogang Xu, Kwan San Hui, ... Wen He
Article 156082
Purchase PDF Article preview

Research article ○ Abstract only
Flow stress characteristics and microstructural evolution of cast superalloy 625 during hot deformation
Ashwin Kumar Godasu, Ujjwal Prakash, Suhrit Mula
Article 156200
Purchase PDF Article preview

Research article ○ Abstract only
Tailoring the mesoporous $ZnMn_2O_4$ spheres as anode materials with excellent cycle stability for sodium-ion batteries
Rasu Muruganantham, Irish Valerie B. Maggay, Jun-Ying Huang, Yan-Gu Lin, ... Wei-Ren Liu
Article 156018
Purchase PDF Article preview

Research article ○ Abstract only
Influence of laser shock peening on the coefficient of thermal expansion of Al (7075)-based hybrid composites
J.T. Wang, L. Xie, Z.G. Wang, H. Gu, ... M.Z. Ge
Article 156088
Purchase PDF Article preview

Research article ○ Abstract only
Revealing the effect of minor Ca and Sr additions on microstructure evolution and mechanical properties of Zn-0.6 Mg alloy during multi-pass equal channel angular pressing
He Huang, Huan Liu, Lisha Wang, Kai Yan, ... Jing Bai
Article 155923
Purchase PDF Article preview

Research article ○ Abstract only
Ir-oxide mediated surface restructure and corresponding impacts on durability of bimetallic NiO_x@Pd nanocatalysts in oxygen reduction reaction
Dinesh Bhalothia, Dai-Ling Tsai, Sheng-Po Wang, Che Yan, ... Po-Chun Chen
Article 156160
Purchase PDF Article preview

Journal of Alloys and Compounds
Supports *open access*

7.6
CiteScore

Double doped cerium-based superhydrophobic layered double hydroxide protective films grown on anodic aluminium surface
Muhammad Ahsan Iqbal, Humaira Asghar, Michele Fedel
Article 156112

Purchase PDF Article preview

Research article ○ Abstract only
N-doped carbon confined $Na_3V_2(PO_4)_3$ derived from an organophosphonic acid as a high-performance cathode for sodium-ion batteries
Yaping Wang, Kangjia Zhao, Kui Wang, Huanhuan Li, ... Long Chen
Article 156118

Purchase PDF Article preview

Research article ○ Abstract only
An enhanced ceramic conversion treatment of Ti6Al4V alloy surface by a pre-deposited thin gold layer
Zhenxue Zhang, Yuejiao Zhang, Xiaoying Li, James Alexander, Hanshan Dong
Article 155867

Purchase PDF Article preview

Research article ○ Abstract only
Synthesis of palladium carbides and palladium hydride in laser heated diamond anvil cells
T. Fedotenko, L. Dubrovinsky, S. Khandarkhaeva, S. Chariton, ... N. Dubrovinskaia
Article 156179

Purchase PDF Article preview

Correspondence ○ Abstract only
Invar alloy@nitrogen doped carbon nanotubes as efficient bifunctional catalyst for lithium-oxygen batteries
Tianwei Li, Huangxu Li, Hongzhong Li, Yangyang Xie, Zhian Zhang
Article 156199

Purchase PDF Article preview

Research article ○ Abstract only
Heterostructures of mesoporous hollow Zn_2SnO_4/SnO_2 microboxes for high-performance acetone sensors
Jie Lu, Yanmei Xie, Fuli Luo, Hao Fu, ... Hongjie Liu
Article 155788

Purchase PDF Article preview

Research article ○ Abstract only
Stability studies and magnetic behaviour of rhodium vanadate
Keka Chakraborty, Mayuresh Mukadam, Aparna Banerjee

Journal of Alloys and Compounds
Supports *open access*

7.6
CiteScore

Articles & Issues About Publish

Research article ○ Abstract only
Improved electrochemical performance of interface modified MoS_2/CNT nano-hybrid and understanding of its lithiation/delithiation mechanism
Kruti K. Halankar, Balaji P. Mandal, Manoj K. Jangid, Amartya Mukhopadhyay, ... A.K. Tyagi
Article 156076
Purchase PDF Article preview

Research article ○ Abstract only
Novel full spectrum photocatalyst based on Pd nanoparticles decorating F doped $(NH_4)_{0.33}WO_3$ nanorods
Qiang Gao, Xiaomei Wu, Yi Kang
Article 155512
Purchase PDF Article preview

Review article ○ Abstract only
Mineral-TiO_2 composites:Preparation and application in papermaking, paints and plastics
Yu Liang, Hao Ding
Article 156139
Purchase PDF Article preview

Research article ○ Abstract only
Effects of N_2-content on formation behavior in AlN thin films studied by NEXAFS: Theory and experiment
Ratchadaporn Supruangnet, Wutthigrai Sailuam, Wutthikrai Busayaporn, Chakkaphan Wattanawikkam, ... Atipong Bootchanont
Article 156128
Purchase PDF Article preview

Research article ○ Abstract only
Ferromagnetic phase transition and anomalies of thermodynamic characteristics of copper-deficient $EuCu_2P_2$ at low temperatures
V.V. Novikov, A.V. Matovnikov, N.V. Mitroshenkov, A.V. Morozov, ... A.V. Shevelkov
Article 156150
Purchase PDF Article preview

Research article ○ Abstract only
Large positive magnetoresistance with high Hall mobility and intercalation of Fe dopants in the quenched Bi_2Te_3 single crystals
Shuo-Hong Wang, Dong Shen, Tien-Wei Yang, I-Nan Chen, ... Li-Min Wang
Article 156153
Purchase PDF Article preview

Journal of Alloys and Compounds
Supports *open access*

7.6
CiteScore

Nitrogen-doped porous carbon composite with three-dimensional conducting network for high rate supercapacitors
Mengmeng Wu, Shixuan Tong, Lili Jiang, Baoquan Hou, ... Lizhi Sheng
Article 156217

Purchase PDF Article preview

Research article ○ Abstract only
Dynamic recrystallization mechanism of γ and α phases during the isothermal compression of γ-TiAl alloy with duplex structure
R.R. Xu, H. Li, M.Q. Li
Article 156089

Purchase PDF Article preview

Research article ○ Abstract only
Physically transient random number generators based on flexible carbon nanotube composite threshold switching
Yanmei Sun, Dianzhong Wen
Article 156144

Purchase PDF Article preview

Research article ○ Abstract only
Influence of $CaO–B_2O_3–SiO_2$ crystallizable glass on microstructure and microwave dielectric of $LiMg_{0.9}Zn_{0.1}PO_4$ ceramics for LTCC substrate applications
Yang Lv, Wanfeng Zhou, Zhaowen Dong, Siqi Yuan, ... Song Cui
Article 156212

Purchase PDF Article preview

Research article ○ Abstract only
Polyol mediated synthesis of anisotropic ZnO nanomaterials and composite with rGO: Application towards hybrid supercapacitor
Sudha Murali, Pradeep Kumar Dammala, Barkha Rani, Ravichandran Santhosh, ... Niroj Kumar Sahu
Article 156149

Purchase PDF Article preview

Journal of Alloys and Compounds
Supports *open access*

7.6
CiteScore

Journal of Alloys and Compounds 844 (2020) 156132

Contents lists available at ScienceDirect

Journal of Alloys and Compounds

journal homepage: http://www.elsevier.com/locate/jalcom

Electrocaloric effect of alkali co-substituted $Sr_{0.6}Ba_{0.4}Nb_2O_6$ ceramics

Arif Kurnia [a], Emriadi [a], Nandang Mufti [b], Zulhadjri [a], Umut Adem [c, *]

[a] Department of Chemistry, Faculty of Mathematics and Natural Sciences, Universitas Andalas, Kampus Limau Manis, Padang, 25163, Indonesia
[b] Department of Physics, Faculty of Mathematics and Natural Sciences, Universitas Negeri Malang, Jl. Semarang 5, Malang, 65145, Indonesia
[c] Department of Materials Science and Engineering, Izmir Institute of Technology, Urla, 35430, Izmir, Turkey

ARTICLE INFO

Article history:
Received 1 May 2020
Received in revised form
2 June 2020
Accepted 18 June 2020
Available online 20 June 2020

Keywords:
Electrocaloric effect
Strontium barium niobate
Tetragonal tungsten bronze
Cation disorder

ABSTRACT

We have investigated the electrocaloric properties of K^+ and Na^+ co-substituted $Sr_{0.6}Ba_{0.4}Nb_2O_6$ (SBN) ceramics using the indirect method. Tetragonal tungsten bronze $(K_{0.5}Na_{0.5})_{2x}(Sr_{0.6}Ba_{0.4})_{5-x}Nb_{10}O_{30}$ (KNSBN) with $x = 0.24$ was synthesized using dual-step sintering. Despite the low amount, K^+ and Na^+ co-substitution resulted in normal ferroelectric behaviour, showing no significant shift in the dielectric maximum temperature of 111 °C with increasing frequency. Maximum electrocaloric temperature change (ΔT) of 0.3 K was observed at an electric field of 30 kV/cm (ΔE) yielding the largest electrocaloric responsivity (ΔT/ΔE) among SBN based ceramics. This relatively large value is in agreement with the larger pyroelectric coefficient of KNSBN compared to SBN based ceramics.

1. Introduction

Recently, solid state cooling based on caloric materials received a lot of attention as an alternative for the conventional vapor compression based cooling technology due to its advantages such as lack of hazardous gases, compact size and high theoretical efficiency of the cooling cycle [1–4]. Among the caloric materials, electrocaloric materials are dielectric materials that show change in their dipolar entropy when an electric field is applied or withdrawn. The change of dipolar entropy upon the application of electric field results in a temperature change under adiabatic conditions; this phenomenon is called the electrocaloric effect [1,5]. The electrocaloric effect is large around the phase transitions in the ferroelectric as well as antiferroelectric materials such as ferroelectric to paraelectric [6], antiferroelectric to ferroelectric [7] or ferroelectric to ferroelectric [8] phase transitions where large entropy changes take place. Ceramic and polymer ferroelectric materials in bulk as well as in thin and thick film forms are studied as electrocaloric materials [4]. Bulk ceramics have larger cooling capacity and larger electrocaloric responsivity than thin film counterparts, suited for the medium to large scale refrigeration systems [9]. Despite the large electrocaloric effect reported for Pb-based systems, due to the toxicity of Pb, research is also focused on Pb-free ferroelectrics for electrocaloric cooling applications. Pb-free systems that are extensively explored include $BaTiO_3$ based systems such as $BaTi_{1-x}Sn_xO_3$ [10], $BaHf_xTi_{1-x}O_3$ [6], $Ba_{0.8}Sr_{0.2}Ti_{1-x}Zr_xO_3$ [11] as well as $Na_{0.5}Bi_{0.5}TiO_3$ [12] and $K_{0.5}Na_{0.5}NbO_3$ [13] based materials.

Tetragonal tungsten bronze (TTB) ceramics have good dielectric, ferroelectric, pyroelectric and piezoelectric properties and versatile applications in electro-optics [14–17]. TTB structure with the general formula $(A1)_2(A2)_4C_4B_{10}O_{30}$, consists of BO_6 octahedra linked by corner sharing, thereby creating three different interstitial sites for the A-site cations (two A1 (square), four A2(pentagonal), and four C(trigonal)) along the *c* axis (inset of Fig. 1) [18]. Due to the presence of these different interstitial sites, combinations of different cations can be introduced to the structure and the properties can be tuned. The [14]structure is called 'stuffed' when all 3 interstitial sites are occupied. When all A1 and A2 sites are occupied, the structure is named 'filled' and if 5 out of 6 total A sites are occupied then it is called 'partially filled' [14] or in many other references 'unfilled' [19]. We prefer to use the 'unfilled' term in this manuscript.

Among the tetragonal bronze family, mainly strontium barium niobate ($Sr_xBa_{1-x}Nb_2O_6$), in short SBN, has been studied for electrocaloric cooling. In SBN, C site is empty and A1 and A2 sites are not fully occupied (5 out of 6 total A sites are occupied) therefore the structure can be considered as 'unfilled'. With the increase of Sr content, SBN shows a transition from normal ferroelectric to relaxor ferroelectric state around $x = 0.5$. Le Goupil et al. studied the

* Corresponding author.
E-mail address: umutadem@iyte.edu.tr (U. Adem).

https://doi.org/10.1016/j.jallcom.2020.156132
0925-8388/

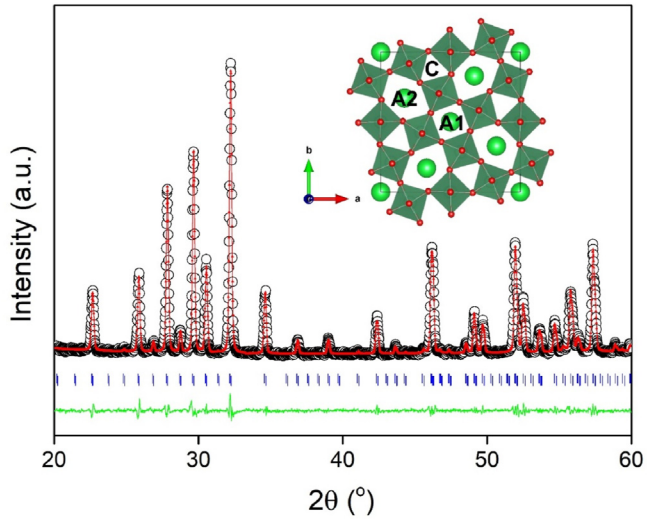

Fig. 1. Le Bail fit of the XRD pattern of the dual-step sintered KNSBN. Observed XRD intensity (circles), calculated intensity (solid line), and the difference of observed and calculated patterns, $y_{obs} - y_{cal}$ (solid line at the bottom). Tick marks represent the positions of allowed Bragg reflections in *P4mm* space group. Inset shows the tetragonal tungsten bronze structure viewed along the *c*-axis.

electrocaloric effect of $Sr_{0.75}Ba_{0.25}Nb_2O_6$ single crystals, which shows relaxor ferroelectric characteristics, using direct measurements. They obtained a maximum ΔT of ≈0.4 K under 10 kV/cm, when the electric field is applied along the polar direction of SBN [20]. Tang et al. [21] studied electrocaloric effect of $Sr_xBa_{1-x}Nb_2O_6$ ceramics ($x = 0.4$, 0.5 and 0.6) and reported that $Sr_{0.6}Ba_{0.4}Nb_2O_6$ has the highest ΔS (0.39 J/kg) and ΔT (0.32 K) under the 60 kV/cm. They also showed that $Sr_{0.6}Ba_{0.4}Nb_2O_6$ composition has the best pyroelectric energy harvesting performance. It is reasonable to expect a material with better pyroelectric properties to show better electrocaloric properties since pyroelectric properties and electrocaloric effect are commensurate [21,22]. To obtain better pyroelectric properties, $Sr_xBa_{1-x}Nb_2O_6$ system was doped with various cations e.g. Y^{3+}, La^{3+}, Ce^{3+}, Pr^{3+}, Nd^{3+}, Sm^{3+}, Eu^{3+}, Gd^{3+}, Tm^{3+}, Dy^{3+}, Er^{3+}, Yb^{3+}, K^+ and Na^+ [23,24]. Yao et al. [23] reported that pyroelectric properties of $Sr_{0.5}Ba_{0.5}Nb_2O_6$ increase with the Gd^{3+} dopant from 49 μC/m^{2}K to 168 μC/m^{2}K at room temperature however the origin of this improvement was not discussed. In another study, $Sr_{0.6}Ba_{0.4}Nb_2O_6$ was doped using two alkali cations K^+ and Na^+ with the formula $(K_{0.5}Na_{0.5})_{2x}(Sr_{0.6}Ba_{0.4})_{5-x}Nb_{10}O_{30}$ ($0.24 \leq x \leq 1.0$) (KNSBN) [24]. The composition with $x = 0.24$ yielded the highest pyroelectric coefficient (p) of 284 μC/m^{2}K at room temperature and the lowest transition temperature at 130 °C among the series. This room temperature p is even larger than that of $Sr_{0.6}Ba_{0.4}Nb_2O_6$ ceramics. More interestingly, even though when the Sr content in $Sr_xBa_{1-x}Nb_2O_6$ exceeds $x \geq 0.5$, a transition from normal ferroelectric to relaxor ferroelectric behavior is induced; in the case of KNSBN, it was shown that normal ferroelectric character is kept even at the lowest Na^+ and K^+ doped composition of $x = 0.24$ [24] as we will discuss later.

In this study, motivated by the normal ferroelectric-like behavior and large pyroelectric coefficient reported earlier, we investigate the electrocaloric properties of $(K_{0.5}Na_{0.5})_{2x}(Sr_{0.6}Ba_{0.4})_{5-x}Nb_{10}O_{30}$ with $x = 0.24$ using the indirect method and report that in agreement with its large pyroelectric coefficient, KNSBN also shows large electrocaloric effect compared to SBN based ceramics. We use a simplified version of the chemical formula in order to compare more easily with the parent $Sr_{0.6}Ba_{0.4}Nb_2O_6$ composition: $(K_{0.5}Na_{0.5})_{0.096}(Sr_{0.6}Ba_{0.4})_{0.952}Nb_2O_6$. Dual step sintering was applied to avoid abnormal grain growth since it has been shown that in the $Sr_xBa_{1-x}Nb_2O_6$ system the liquid phase can easily form during the sintering process which might cause abnormal grain growth [25–27]. It is known that abnormal grain growth might result in deterioration of the dielectric and ferroelectric properties [26,28]. While we focus on the electrocaloric properties of the sample obtained by dual-step sintering, we also provide a comparison of the microstructure as well as dielectric and ferroelectric properties of this sample with the sample obtained using conventional sintering.

2. Experimental

KNSBN was prepared from K_2CO_3 (≥99.0%, Isolab Chemicals), Na_2CO_3 (≥99.8%, Isolab Chemicals), $SrCO_3$ (≥99.5%, Enteknomaterials), $BaCO_3$ (≥99.5%, Enteknomaterials), and Nb_2O_5 (≥99.5%, Alfa Aesar). Starting powders were mixed in ethanol using planetary ball milling (Retsch PM 100) in a nalgene bottle with zirconia balls for 18 h. The mixed powder was dried and calcined at 1100 °C for 6 h. The calcined powder was mixed with 5 wt% polyvinyl alcohol as the binder and formed into the pellets using uniaxial pressing. Binder burnout was performed at 600 °C for 5 h with a heating rate of 1 °C/min. For the dual-step sintered sample, first pre-sintering was carried out at 1150 °C for 4 h with a heating rate of 5 °C/min. Then, the sample was again sintered at 1270 °C for 2 h with a heating rate of 5 °C/min. Pre-sintering step was not applied for the conventionally sintered sample i.e. after binder burnout the sample was directly sintered at 1270 °C for 2 h with a heating rate of 5 °C/min. The density of pellets were measured using the Archimedes method. Phase analysis of samples was done by X-ray diffraction (Panalytical X'Pert Pro) and unit cell parameters were obtained from Le Bail fits using Rietica [29]. Polishing and thermal etching were applied for microstructural observation. The morphology of the sample was analyzed by a scanning electron microscope (SEM, Quanta 250 FEG). The average grain size was calculated using the linear intercept method.

For the electrical measurements, both sides of the pellet were coated with silver epoxy. The dielectric constant of the sample was measured using an LCR-meter (Keysight E4980AL) between 50 and 200 °C at 100 Hz, 1 kHz, 10 kHz and 100 kHz. Ferroelectric hysteresis loops were measured using a commercial ferroelectric tester (Aixacct TF Analyzer 1000) at 10 Hz between room temperature and 160 °C.

Electrocaloric temperature change (ΔT) of the sample was calculated using the indirect method based on Maxwell's equations (Eq. (1)).

$$\Delta T = -\frac{1}{\rho}\int_{E_1}^{E_2}\frac{T}{c}\left(\frac{\partial P}{\partial T}\right)_E dE \quad (1)$$

where P is the electrical polarization, E1, E2 are initial and final electric field, c is the heat capacity, ρ is the density and T is the temperature.

3. Results and discussion

3.1. Structural characterization

Le Bail fit to the X-ray diffraction spectra of dual-step sintered KNSBN is shown in Fig. 1. All observed peaks belong to the tetragonal tungsten bronze structure. Lattice parameters were obtained from the Le Bail fit using the tetragonal tungsten bronze structure of SBN with the space group *P4mm* as the standard [30]. The fit

quality was good, evidenced by the difference curve and the low R_{wp} of 4.44%. Lattice parameters *a* and *c* were obtained as 12.449(6) Å and 3.933(9) Å, respectively, in agreement with KNSBN compositions reported in Refs. [24].

Fig. 2 shows SEM micrograph of the surface of the sample sintered using dual step sintering. While the abnormal grain growth could be prevented: i.e. giant grains of 100 μm size were not observed [27], grain size distribution is broad and not homogeneous. Similar microstructure was reported for some SBN compositions synthesized using dual sintering [31]. The average grain size was estimated to be ~2 μm(Fig. 2). The measured density of the sample was ~91% of the theoretical density. We note that following conventional sintering with the same calcination temperature and the single sintering step at 1270 °C for 2 h, we have obtained a microstructure (Fig.S2(b)) with cracks and inhomogeneities, suggesting liquid phase formation and abnormal grain growth. Adding a pre-sintering step approximately 100 °C below the normal sintering temperature (i.e. dual-step sintering) is reported to prevent liquid phase formation since the liquid phase formation is triggered by incomplete calcination [27]. Comparison of the sintering profiles and microstructures of the two samples obtained using conventional and dual-step sintering is provided in the supplementary material (Fig. S1 and S2).

3.2. Dielectric properties

Dielectric constant (ε) and dielectric loss (tan δ) of dual-step sintered KNSBN in the temperature range of 50–200 °C and at various frequencies (100 Hz, 1 kHz, 10 kHz, and 100 kHz) are presented in Fig. 3. Dielectric constant shows a broad peak at the transition temperature (*Tm*) around 111 °C. In agreement with the study of Yao et al. [24], dielectric peak position does not shift significantly towards higher temperatures with increasing frequency, pointing to a normal ferroelectric with diffuse phase transition character rather than a ferroelectric relaxor. This is in contrast to what has been reported for $Sr_{0.6}Ba_{0.4}Nb_2O_6$ ceramics, where a clear shift in the broad dielectric maximum to higher temperatures is reported [32,33]. The maximum value of our dielectric constant is smaller than that reported in Ref. [24]. This could be due to the slightly smaller average grain size of our samples (2 μm compared to 5 μm). It is well known that the larger grain size can yield better dielectric and ferroelectric properties [27,34]. T_m we obtained is also lower than that reported in the earlier report [24]. This lower transition temperature might have resulted from the slightly lower grain size of our samples. It was reported that Ce doping suppresses grain growth in $Sr_{0.5}Ba_{0.5}Nb_2O_6$ ceramics and in turn causes a significant decrease in Curie temperature due to the larger internal stress in fine grained samples [35]. The dielectric loss of the sample decreased with increasing temperature until the temperature of the dielectric maximum and then reaches a plateau for 10 and 100 kHz. The temperature of the plateau shifts to higher temperatures with increasing frequency. At 100 Hz and 1 kHz, an increase of dielectric loss at high temperatures was observed which might be related to the increasing dc conductivity at these temperatures [36]. Dielectric loss was smaller than 0.022 over the whole temperature range. Comparison of the temperature dependence of the dielectric constant of the samples obtained using conventional and dual-step sintering is provided in Fig. S3. Dielectric constant of the dual-step sintered sample is larger than that of the conventionally sintered one, while its dielectric maximum temperature is lower. Similar behaviour was reported for SBN ceramics and explained in terms of the internal stress developed in fine-grained samples (obtained by dual-step sintering) during cooling [27].

As mentioned in the introduction section, in the SBN system, Sr^{2+} and Ba^{2+} occupy A1 and A2 sites while C site of TTB structure is empty. Five of the six A-site positions are occupied: A1 sites are filled by Sr^{2+} ions, whereas both Sr^{2+} and Ba^{2+} can occupy A2 site. There is a strong correlation between the occupancy of the A1 and A2 sites and the relaxor ferroelectric character of the material. Normal ferroelectric behavior with no frequency dispersion of the dielectric peak was observed for $Sr_xBa_{1-x}Nb_2O_6$ when $x = 0.20$ (Sr/Ba = 1/4). In that case, four A2 sites are occupied by Ba^{2+} while one of the two A1 sites is occupied by one Sr^{2+} and thus, an ordered and even distribution of ions is obtained [19]. When the composition moves away from $x = 0.25$, cation distribution becomes disordered and relaxor ferroelectric behavior is observed with the signature of frequency dispersion of the dielectric maximum. The strength of frequency dispersion in $Sr_xBa_{1-x}Nb_2O_6$ system increases with strontium content [19,37]. It has been established that the origin of the relaxor behavior in SBN is the 'quenched electric random fields related to randomly distributed vacancies on the A-sites' [38]. One way to decrease the disorder and frequency dispersion is introducing alkali ions such as Na^+ and K^+. Introduction of Na^+ and K^+ to the structure causes the filling of vacant A1 and A2 sites since for each divalent cation, two monovalent Na^+ or K^+ are introduced while small C sites remain unoccupied [33,39]. This decrease in the vacant sites is reported to cause the suppression of relaxor

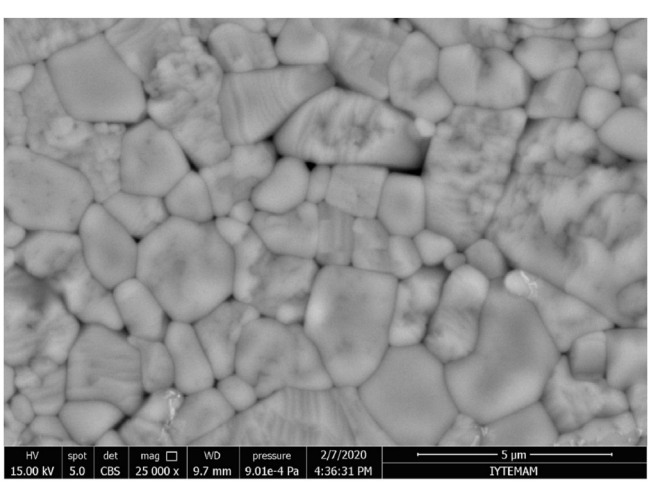

Fig. 2. SEM surface micrograph of the dual-step sintered KNSBN.

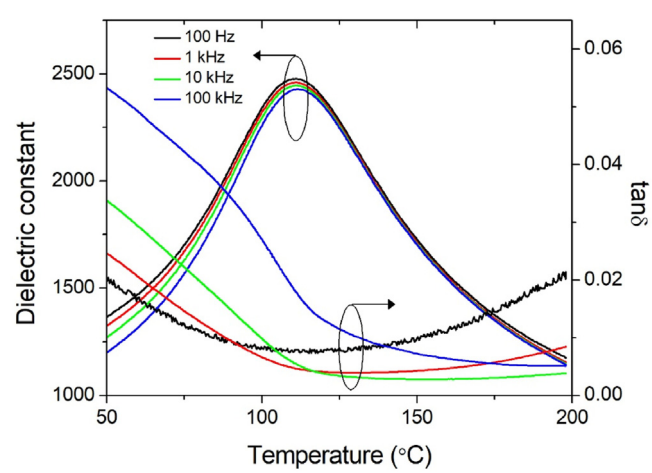

Fig. 3. Temperature dependence of the dielectric constant and dielectric loss of dual-step sintered KNSBN at different frequencies.

ferroelectric properties and induces diffuse phase transition [33]. In our case, the amount of Na^+ or K^+ introduced at the A-sites is quite small however is enough to decrease the frequency dispersion and induce normal ferroelectric behavior with diffuse phase transition character.

3.3. Ferroelectric and electrocaloric properties

In Fig. 4 ferroelectric hysteresis loops of dual-step sintered KNSBN measured at 10 Hz and different temperatures are shown. At room temperature, the sample exhibits a typical hysteresis loop. Hysteresis loops become slimmer with increasing temperature and at and above $T_m = 111$ °C, they fully close-up and at the highest measurement temperature of 160 °C an almost linear loop is observed, suggesting that the paraelectric state is reached. The value of the maximum polarization is comparable to SBN ceramics [40] when compared at the same electric field. A comparison of the hysteresis loops of the samples obtained using conventional and dual-step sintering is provided in Fig. S4. It can be observed that while the maximum polarization of the dual-step sintered sample is larger, its coercive field is smaller than that of the conventionally sintered sample. These differences are related to the higher density (91 vs. 86%), better crystallinity and relatively homogeneous microstructure of the dual-step sintered sample.

Electrocaloric temperature change (ΔT) of the dual-step sintered sample was calculated by the indirect method, using equation (1). For the calculation, first $\left(\frac{\partial P}{\partial T}\right)_E$ was obtained. In order to do this, the temperature dependence of the electrical polarization at different electric fields were plotted using the data from the upper branches of the hysteresis loops, as illustrated in Fig. 5(a). The curves were fitted with 6th order polynomials and then the fitted curve is differentiated. ΔT was then calculated using equation (1). In the calculation, measured density (ρ) of 4.81 g/cm^3 was used. Heat capacity (c) value of 330 J/kgK was taken from Ref. [24] which is the value reported for the KNSBN of the same composition. The temperature evolution of ΔT under different electric fields is shown in Fig. 5(b). ΔT shows a broad peak at around $T_m = 111$ °C under 10 kV/cm ΔT peak shifts to higher temperatures as the electric field is increased. ΔT reaches 0.3 K under 30 kV/cm at around 133 °C and the calculated electrocaloric responsivity or strength ($\Delta T/\Delta E$) is 0.1 K*mm/kV at this temperature. Even though this value is modest among Pb-free ceramics, it is the largest among SBN based ceramics as we discuss below. We note that the dual-step sintered sample underwent dielectric breakdown above 30 kV/cm. This relatively low dielectric breakdown strength is likely to originate from the slightly low density of the sample since density is one of the key factors controlling the breakdown strength [41]. Conventionally sintered sample had even lower breakdown strength as it underwent dielectric breakdown at high temperatures. Therefore its electrocaloric property measurements couldn't be completed. This must be caused by its inhomogenous microstructure.

In Table 1, the electrocaloric properties of KNSBN are compared with different SBN compositions in ceramic and single crystal form. In order to compare the electrocaloric effect, $\Delta T/\Delta E$ values for each material are listed. In addition to the measurement method, the nature of the material i.e. whether the material behaves as a ferroelectric relaxor or normal ferroelectric is also included in the table. KNSBN shows better electrocaloric responsivity than all SBN ceramic compositions reported so far however as expected single crystal SBN compositions outplay KNSBN ceramic. We stress that all SBN compositions listed in Table 1 are mostly relaxor ferroelectrics unlike the KNSBN composition we report here. Indirect measurement of electrocaloric effect based on Maxwell's relations is not accurate for relaxor ferroelectrics nevertheless it is still used to estimate the electrocaloric effect. Direct measurement was shown to yield larger electrocaloric temperature change for many ceramics compared to the indirect method [42–44]. Large ΔT of KNSBN is in accordance with its large room temperature pyroelectric coefficient (p) reported by Yao et al. (284 μC/m^{2}K). KNSBN's room temperature pyroelectric coefficient is greater than that of $Sr_{0.5}Ba_{0.5}Nb_2O_6$ ceramics (200 μC/m^{2}K) [17], which has the largest p among SBN compositions. And this difference does not originate from a

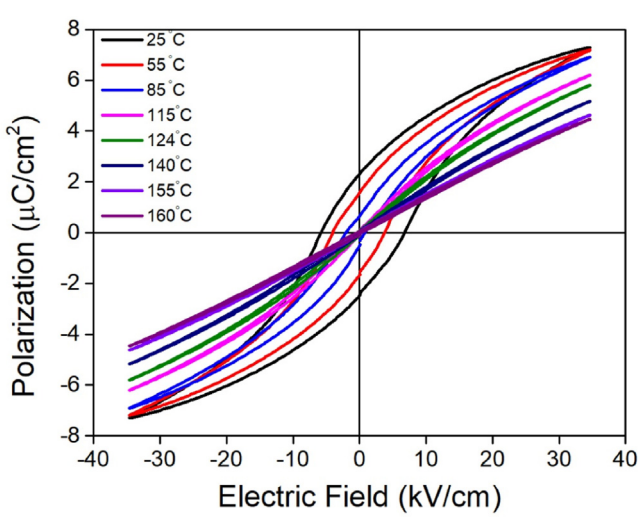

Fig. 4. Ferroelectric hysteresis loops of the dual-step sintered KNSBN at different temperatures measured at 10 Hz.

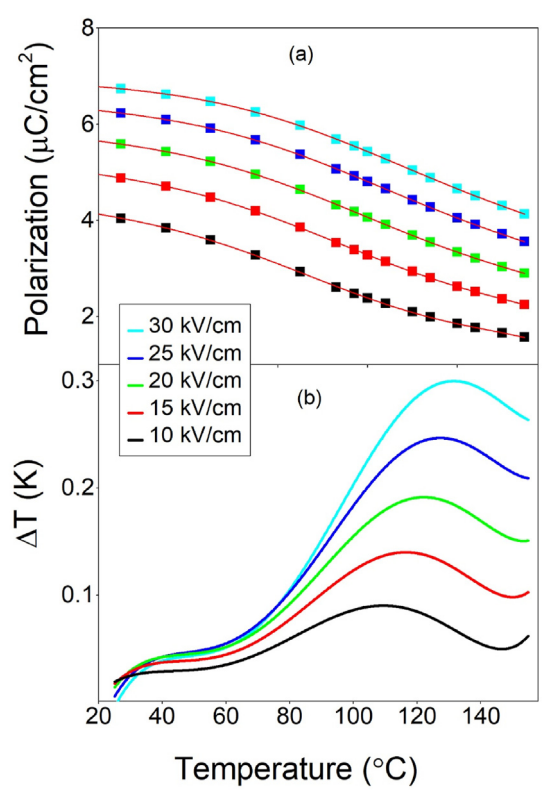

Fig. 5. (a) Electrical polarization of the dual-step sintered KNSBN as a function of temperature at different electric fields. The solid line is a fit to a sixth-degree polynomial, (b) Electrocaloric temperature change (ΔT) of dual-step sintered KNSBN as a function of temperature at different electric fields.

Table 1
Comparison of the electrocaloric properties for different SBN related materials.

Material	Form	Tc or Tm (°C)	ΔT (K)	E (kV/cm)	ΔT/ΔE (K*mm/kV)	Method/Material Type	Ref.
$Sr_{0.5}Ba_{0.5}Nb_2O_6$	ceramic	50	0.35	100	0.035	indirect/relaxor	[47]
$Sr_{0.6}Ba_{0.4}Nb_2O_6$	ceramic	134	0.32	60	0.053	indirect/relaxor	[21]
$Sr_{0.698}Gd_{0.002}Ba_{0.3}Nb_2O_6$	ceramic	40	0.085	15	0.056	indirect/relaxor	[48]
$Sr_{0.6}Ba_{0.4}Nb_2O_6$	Single crystal	<35	0.42	10	0.42	direct/relaxor	[20]
$Sr_{0.61}Ba_{0.39}Nb_2O_6$ +1.4 %Ce	Single crystal	<30	0.85	28	0.303	direct/relaxor	[49]
KNSBN	**ceramic**	**133**	**0.30**	**30**	**0.1**	**indirect/normal ferroelectric**	**This work**

proximity effect to the Curie temperature. $Sr_{0.5}Ba_{0.5}Nb_2O_6$ ceramics has a T_C of approximately 80 °C [17] which is lower than that of KNSBN. This difference between p of KNSBN and SBN ceramics points out to a sharper change of electrical polarization in KNSBN and partially accounts for the large ΔT obtained in this study. The difference in ΔT between single crystals and ceramics can be anticipated by looking at the large room temperature value of p of the $Sr_{0.5}Ba_{0.5}Nb_2O_6$ single crystal: 550 μC/m^{2}K [45]. SBN has strongly anisotropic electrical properties and is polar only along [001] direction. In ceramics, randomly oriented grains result in an average value of all crystallographic directions which causes a decrease in the pyroelectric coefficient.

We suggest that the origin of the electrocaloric effect and the large pyroelectric coefficient in KNSBN must be related to the stabilization of ferroelectricity upon K^+ and Na^+ co-substitution. It has been reported that remanent polarization increases as the amount of K^+ and Na^+ increases in KNSBN ceramics [24], which is an indication of the stabilization of ferroelectricity upon doping. In our case, we also observe a relatively large remanent polarization, an increase in the Curie temperature compared to undoped $Sr_{0.6}Ba_{0.4}Nb_2O_6$ as well as dissappearance of the shift of dielectric maximum with increasing frequency; all of which support the stabilization of the ferroelectricity. A similar increase of remanent polarization was observed in $Ca_xSr_{0.3-x}Ba_{0.7}Nb_2O_6$ ceramics where Ca^{2+} doping was suggested to stabilize the ferroelectricity of the material, evidenced by an increase in Curie temperature and remanent polarization with the doping. In addition, the pyroelectric coefficient also increased with increasing Ca^{2+} content [46]. Based on these reports and the observation of normal ferroelectric behavior in our KNSBN, we suggest the relatively large electrocaloric responsivity we measure on KNSBN as well as the previously reported large pyroelectric coefficient, must be related to the stabilization of ferroelectricity with doping. To better understand the origin of large p and electrocaloric responsivity of KNSBN ceramics, however, more work on the possible correlation between the filling of A-site positions with K^+ and Na^+ and the increase in the pyroelectric coefficient and preferably direct measurement of the electrocaloric effect to compare the electrocaloric temperature change of SBN and KNSBN, are necessary.

4. Conclusions

We have investigated the electrocaloric properties of K^+ and Na^+ co-doped SBN. Despite the low amount of alkali doping, KNSBN showed normal ferroelectric like behavior with no significant shift of dielectric maximum temperature with increasing frequency. KNSBN shows a maximum ΔT of 0.3 K under 30 kV/cm which corresponds to an electrocaloric responsivity of 0.1 K*mm/kV around 130 °C. This value is larger than those of SBN ceramics and is in agreement with the larger pyroelectric coefficient value of KNSBN compared to SBN ceramics. We suggest that the relatively large ΔT and p originates from the stabilization of ferroelectricity upon doping.

CRediT authorship contribution statement

Arif Kurnia: Data curation, Writing - original draft. **Emriadi:** Writing - review & editing. **Nandang Mufti:** Supervision, Writing - review & editing. **Zulhadjri:** Supervision, Writing - review & editing. **Umut Adem:** Conceptualization, Supervision, Writing - review & editing.

Declaration of competing interest

The authors declare that they have no known competing financial interests or personal relationships that could have appeared to influence the work reported in this paper.

Acknowledgments

This work was supported by the Ministry of Research, Technology and Higher Education of the Republic of Indonesia through the PMDSU Scholarship (Grant number 050/SP2H/LT/DRPM/2018) and the PKPI-PMDSU Scholarship (Grant number 1406.53/D3/PG/2018). The authors thank İzmir Institute of Technology's Center for Materials Research for XRD and SEM experiments. One of the authors (AK) thanks Merve Karakaya, Meriç Güvenç and Melike Tokkan for their help with the experiments and fruitful discussions.

Appendix A. Supplementary data

Supplementary data to this article can be found online at https://doi.org/10.1016/j.jallcom.2020.156132.

References

[1] S.-G. Lu, Q. Zhang, Electrocaloric materials for solid-state refrigeration, Adv. Mater. 21 (2009) 1983–1987, https://doi.org/10.1002/adma.200802902.
[2] L. Luo, X. Jiang, Y. Zhang, K. Li, Electrocaloric effect and pyroelectric energy harvesting of (0.94−x)$Na_{0.5}Bi_{0.5}TiO_3$-0.06$BaTiO_3$-x$SrTiO_3$ ceramics, J. Eur. Ceram. Soc. 37 (2017) 2803–2812, https://doi.org/10.1016/j.jeurceramsoc.2017.02.047.
[3] A.S. Mischenko, Q. Zhang, J.F. Scott, R.W. Whatmore, N.D. Mathur, Giant electrocaloric effect in thin-film $PbZr_{0.95}Ti_{0.05}O_3$, Science 311 (2006) 1270–1271, https://doi.org/10.1126/science.1123811.
[4] K.S. Srikanth, R. Vaish, Enhanced electrocaloric, pyroelectric and energy storage performance of $BaCe_xTi_{1-x}O_3$ ceramics, J. Eur. Ceram. Soc. 37 (2017) 3927–3933, https://doi.org/10.1016/j.jeurceramsoc.2017.04.058.
[5] M. Valant, Electrocaloric materials for future solid-state refrigeration technologies, Prog. Mater. Sci. 57 (2012) 980–1009, https://doi.org/10.1016/j.pmatsci.2012.02.001.
[6] J. Li, D. Zhang, S. Qin, T. Li, M. Wu, D. Wang, Y. Bai, X. Lou, Large room-temperature electrocaloric effect in lead-free $BaHf_xTi_{1-x}O_3$ ceramics under low electric field, Acta Mater. 115 (2016) 58–67, https://doi.org/10.1016/j.actamat.2016.05.044.
[7] M. Wu, D.S. Song, G. Vats, S.C. Ning, M.Y. Guo, D.W. Zhang, D.Q. Xue, S.J. Pennycook, X.J. Lou, Defect-controlled electrocaloric effect in $PbZrO_3$ thin films, J. Mater. Chem. C. 6 (2018) 10332–10340, https://doi.org/10.1039/c8tc03965h.
[8] M. Marathe, D. Renggli, M. Sanlialp, M.O. Karabasov, V.V. Shvartsman, D.C. Lupascu, A. Grünebohm, C. Ederer, Electrocaloric effect in $BaTiO_3$ at all three ferroelectric transitions: anisotropy and inverse caloric effects, Phys. Rev. B 96 (2017), 014102, https://doi.org/10.1103/PhysRevB.96.014102.
[9] R. Kumar, S. Singh, Enhanced electrocaloric response and high energy-storage properties in lead-free (1-x)$(K_{0.5})NbO_3$ - x$SrZrO_3$ nanocrystalline ceramics,

J. Alloys Compd. 764 (2018) 289–294, https://doi.org/10.1016/j.jallcom.2018.06.083.
[10] Z.D. Luo, D.W. Zhang, Y. Liu, D. Zhou, Y.G. Yao, C.Q. Liu, B. Dkhil, X.B. Ren, X.J. Lou, Enhanced electrocaloric effect in lead-free $BaTi_{1-x}Sn_xO_3$ ceramics near room temperature, Appl. Phys. Lett. 105 (2014) 102904, https://doi.org/10.1063/1.4895615.
[11] K. Şanlı, U. Adem, Electrocaloric properties of $Ba_{0.8}Sr_{0.2}Ti_{1-x}Zr_xO_3$ ($0 \leq x \leq 0.1$) system: the balance between the nature of the phase transition and phase coexistence, Ceram. Int. 46 (2020) 2213–2219, https://doi.org/10.1016/j.ceramint.2019.09.206.
[12] W.P. Cao, W.L. Li, D. Xu, Y.F. Hou, W. Wang, W.D. Fei, Enhanced electrocaloric effect in lead-free NBT-based ceramics, Ceram. Int. 40 (2014) 9273–9278, https://doi.org/10.1016/j.ceramint.2014.01.149.
[13] J. Koruza, B. Rozic, G. Cordoyiannis, B. Malic, Z. Kutnjak, Large electrocaloric effect in lead-free $K_{0.5}Na_{0.5}NbO_3$-$SrTiO_3$ ceramics, Appl. Phys. Lett. 106 (2015) 4, https://doi.org/10.1063/1.4921744.
[14] J.R. Oliver, R.R. Neurgaonkar, L.E. Cross, Ferroelectric properties of tungsten bronze morphotropic phase boundary systems, J. Am. Ceram. Soc. 72 (1989) 202–211, https://doi.org/10.1111/j.1151-2916.1989.tb06102.x.
[15] R.R. Neurgaonkar, W.K. Cory, Progress in photorefractive tungsten bronze crystals, J. Opt. Soc. Am. B 3 (1986) 274–282, https://doi.org/10.1364/JOSAB.3.000274.
[16] B. Yang, L. Wei, X. Chao, Z. Wang, Z. Yang, Role of structural modulation in electrical properties of tungsten bronze $(Ca_{0.28}Ba_{0.72})_{2.5-0.5x}Na_xNb_5O_{15}$ ceramics, J. Alloys Compd. 632 (2015) 368–375, https://doi.org/10.1016/j.jallcom.2015.01.247.
[17] J. Zhang, G. Wang, F. Gao, C. Mao, F. Cao, X. Dong, Influence of Sr/Ba ratio on the dielectric, ferroelectric and pyroelectric properties of strontium barium niobate ceramics, Ceram. Int. 39 (2013) 1971–1976, https://doi.org/10.1016/j.ceramint.2012.08.048.
[18] M. Aftabuzzaman, M.A. Helal, R. Paszkowski, J. Dec, W. Kleemann, S. Kojima, Electric field and aging effects of uniaxial ferroelectrics $Sr_xBa_{1-x}Nb_2O_6$ probed by Brillouin scattering, Sci. Rep. 7 (2017) 11615, https://doi.org/10.1038/s41598-017-10985-9.
[19] C.J. Huang, K. Li, X.Q. Liu, X.L. Zhu, X.M. Chen, Effects of A1/A2-sites occupancy upon ferroelectric transition in $(Sr_xBa_{1-x})Nb_2O_6$ tungsten bronze ceramics, J. Am. Ceram. Soc. 97 (2014) 507–512, https://doi.org/10.1111/jace.12659.
[20] F. Le Goupil, A.K. Axelsson, L.J. Dunne, M. Valant, G. Manos, T. Lukasiewicz, J. Dec, A. Berenov, N.M.N. Alford, Anisotropy of the electrocaloric effect in lead-free relaxor ferroelectrics, Adv. Energy Mater. 4 (2014) 1301688, https://doi.org/10.1002/aenm.201301688.
[21] H. Tang, X.-G. Tang, M.-D. Li, Q.-X. Liu, Y.-P. Jiang, Pyroelectric energy harvesting capabilities and electrocaloric effect in lead-free $Sr_xBa_{1-x}Nb_2O_6$ ferroelectric ceramics, J. Alloys Compd. 791 (2019) 1038–1045, https://doi.org/10.1016/j.jallcom.2019.03.385.
[22] S. Zeng, X. Tang, Q. Liu, Y. Jiang, M. Li, W. Li, Z. Tang, Electrocaloric effect and pyroelectric properties in Ce-doped $BaCe_xTi_{1-x}O_3$ ceramics, J. Alloys Compd. 776 (2018) 731–739, https://doi.org/10.1016/j.jallcom.2018.10.293.
[23] Y. Yao, C.L. Mak, K.H. Wong, S. Lu, Z. Xu, Effects of rare-earth dopants on the ferroelectric and pyroelectric properties of Strontium Barium Niobate Ceramics, Int. J. Appl. Ceram. Technol. 6 (2009) 671–678, https://doi.org/10.1111/j.1744-7402.2008.02308.x.
[24] Y.B. Yao, C.L. Mak, B. Ploss, Phase transitions and electrical characterizations of $(K_{0.5}Na_{0.5})_{2x}(Sr_{0.6}Ba_{0.4})_{5-x}Nb_{10}O_{30}$ (KNSBN) ceramics with "unfilled" and ' filled ' tetragonal tungsten – bronze (TTB) crystal structure, J. Eur. Ceram. Soc. 32 (2012) 4353–4361, https://doi.org/10.1016/j.jeurceramsoc.2012.07.034.
[25] T.-T. Fang, E. Chen, W.-J. Lee, On the discontinuous grain growth of $Sr_xBa_{1-x}Nb_2O_6$ ceramics, J. Eur. Ceram. Soc. 20 (2000) 527–530, https://doi.org/10.1016/s0955-2219(99)00178-8.
[26] H. Lee, R. Freer, Abnormal grain growth and liquid-phase sintering in $Sr_{0.6}Ba_{0.4}Nb_2O_6$ (SBN40) ceramics, J. Mater. Sci. 33 (1998) 1703–1708, https://doi.org/10.1023/A:1004312128588.
[27] H.Y. Lee, R. Freer, The mechanism of abnormal grain growth in $Sr_{0.6}Ba_{0.4}Nb_2O_6$ ceramics, J. Appl. Phys. 81 (1997) 376–382, https://doi.org/10.1063/1.364122.
[28] J. Li, Y. Pu, Z. Wang, J. Dai, A comparative study of $Sr_{0.7}Ba_{0.3}Nb_2O_6$ relaxor ferroelectric ceramics prepared by conventional and microwave sintering techniques, Ceram. Int. 39 (2013) 5069–5075, https://doi.org/10.1016/j.ceramint.2012.12.001.
[29] J.C. Howard, B.A. Hunter, B.A. Rietica, A computer program for Rietvield analysis of X-ray and neutron powder diffarction pattern, Lucas Height, Res. Lab. 1 (1998) 27, https://doi.org/10.3938/jkps.66.1077.
[30] S. Podlozhenov, H.A. Graetsch, J. Schneider, M. Ulex, M. Wöhlecke, K. Betzler, Structure of strontium barium niobate $Sr_xBa_{1-x}Nb_2O_6$ (SBN) in the composition range $0.32 \leq x \leq 0.82$, Acta Crystallogr. Sect. B Struct. Sci. B62 (2006) 960–965, https://doi.org/10.1107/S0108768106038869.
[31] M.S. Kim, J.H. Lee, J.J. Kim, H.Y. Lee, S.H. Cho, Origin of abnormal grain growth in tungsten bronze structured ferroelectric $Sr_xBa_{1-x}Nb_2O_6$ ceramics, Japanese J. Appl. Physics, Part 1 Regul. Pap. Short Notes Rev. Pap. 41 (2002) 7048–7052, https://doi.org/10.1143/JJAP.41.7048.
[32] Y. Zhao, J. Wang, L. Zhang, X. Shi, S. Liu, D. Zhang, Relaxor transition and properties of Mn-doped $Sr_xBa_{1-x}Nb_2O_6$ ferroelectric ceramics, Ceram. Int. 42 (2016) 16697–16702, https://doi.org/10.1016/j.ceramint.2016.07.120.
[33] A. Belous, O. V'Yunov, D. Mishchuk, S. Kamba, D. Nuzhnyy, Effect of vacancies on the structural and relaxor properties of $(Sr,Ba,Na)Nb_2O_6$, J. Appl. Phys. 102 (2007), 014111, https://doi.org/10.1063/1.2752551.
[34] W. Cai, C. Fu, J. Gao, H. Chen, Effects of grain size on domain structure and ferroelectric properties of barium zirconate titanate ceramics, J. Alloys Compd. 480 (2009) 870–873, https://doi.org/10.1016/j.jallcom.2009.02.049.
[35] L. Wang, W. Sui, S. Luan, R. Song, J. Tan, Sintering behavior and dielectric properties of Ce doped strontium barium niobate ceramics with silica sintering additive, Mater. Chem. Phys. 134 (2012) 531–535, https://doi.org/10.1016/j.matchemphys.2012.03.028.
[36] P. Dhak, D. Dhak, M. Das, P. Pramanik, Dielectric and impedance spectroscopy study of $Ba_{0.8}Bi_{2.133}Nb_{1.6}Ta_{0.4}O_9$ ferroelectric ceramics, prepared by chemical route, J. Mater. Sci. Mater. Electron. 22 (2011) 1750–1760, https://doi.org/10.1007/s10854-011-0358-1.
[37] I.A. Santos, D.U. Spínola, D. Garcia, J.A. Eiras, Dielectric behavior and diffuse phase transition features of rare earth doped $Sr_{0.61}Ba_{0.39}Nb_2O_6$ ferroelectric ceramics, J. Appl. Phys. 92 (2002) 3251–3256, https://doi.org/10.1063/1.1481210.
[38] V.V. Shvartsman, W. Kleemann, T. Łukasiewicz, J. Dec, Nanopolar structure in $Sr_xBa_{1-x}Nb_2O_6$ single crystals tuned by Sr/Ba ratio and investigated by piezoelectric force microscopy, Phys. Rev. B Condens. Matter 77 (2008), 054105, https://doi.org/10.1103/PhysRevB.77.054105.
[39] A. Surmin, P. Fertey, D. Schaniel, T. Woike, Modulated structure of potassium sodium strontium barium niobates (KNSBN): harmonic solution, Acta Crystallogr. Sect. B Struct. Sci. B62 (2006) 228–235, https://doi.org/10.1107/S0108768106001510.
[40] C.J. Huang, K. Li, S.Y. Wu, X.L. Zhu, X.M. Chen, Variation of ferroelectric hysteresis loop with temperature in $Sr_xBa_{1-x}Nb_2O_6$ unfilled tungsten bronze ceramics, J. Mater. 1 (2015) 146–152, https://doi.org/10.1016/j.jmat.2015.02.004.
[41] L. Zhao, Q. Liu, J. Gao, S. Zhang, J.F. Li, Lead-free antiferroelectric silver niobate tantalate with high energy storage performance, Adv. Mater. 29 (2017) 1701824, https://doi.org/10.1002/adma.201701824.
[42] X.D. Jian, B. Lu, D.D. Li, Y.B. Yao, T. Tao, B. Liang, J.H. Guo, Y.J. Zeng, J. Le Chen, S.G. Lu, Direct measurement of large electrocaloric effect in $Ba(Zr_xTi_{1-x})O_3$ ceramics, ACS Appl. Mater. Interfaces 10 (2018) 4801–4807, https://doi.org/10.1021/acsami.7b15933.
[43] X.D. Jian, B. Lu, D.D. Li, Y.B. Yao, T. Tao, B. Liang, X.W. Lin, J.H. Guo, Y.J. Zeng, S.G. Lu, Enhanced electrocaloric effect in Sr^{2+}-modified lead-free $BaZr_xTi_{1-x}O_3$ ceramics, ACS Appl. Mater. Interfaces 11 (2019) 20167–20173, https://doi.org/10.1021/acsami.9b04036.
[44] P. Wu, X. Lou, J. Li, T. Li, H. Gao, M. Wu, S. Wang, X. Wang, J. Bian, X. Hao, Direct and indirect measurement of electrocaloric effect in lead-free (100-x) $Ba(Hf_{0.2}Ti_{0.8})O_3$-$x(Ba_{0.7}Ca_{0.3})TiO_3$ ceramics near multi-phase boundary, J. Alloys Compd. 725 (2017) 275–282, https://doi.org/10.1016/j.jallcom.2017.07.103.
[45] C.R. Bowen, J. Taylor, E. Leboulbar, D. Zabek, A. Chauhan, R. Vaish, Pyroelectric materials and devices for energy harvesting applications, Energy Environ. Sci. 7 (2014) 3836–3856, https://doi.org/10.1039/c4ee01759e.
[46] H. Chen, S. Guo, X. Dong, F. Cao, C. Mao, G. Wang, $Ca_xSr_{0.3-x}Ba_{0.7}Nb_2O_6$ lead-free pyroelectric ceramics with high depoling temperature, J. Alloys Compd. 695 (2017) 2723–2729, https://doi.org/10.1016/j.jallcom.2016.11.192.
[47] T. Chen, S.Y. Wu, X.Q. Liu, X.M. Chen, A novel sol-gel route to synthesize $(Sr_{0.5}Ba_{0.5})Nb_2O_6$ ceramics with enhanced electrocaloric effect, J. Adv. Dielectr. 7 (2017) 1750012, https://doi.org/10.1142/S2010135X17500126.
[48] A. V Es'kov, S.A. Anokhin, M.T. Bui, O. V Pakhomov, A.A. Semenov, P.Y. Belyavskiy, A.B. Ustinov, Investigation of the electrocaloric effect in strontium barium niobate (SBN) ceramics with rare-earth dopants, J. Phys. Conf. Ser. 1038 (2018) 12115, https://doi.org/10.1088/1742-6596/1038/1/012115.
[49] F. Le Goupil, A.-K. Axelsson, M. Valant, T. Lukasiewicz, J. Dec, A. Berenov, N.M. Alford, Effect of Ce doping on the electrocaloric effect of $Sr_xBa_{1-x}Nb_2O_6$ single crystals, Appl. Phys. Lett. 104 (2014) 222911, https://doi.org/10.1063/1.4881842.